Article

J. Biol. Regul. Homeost. Agents. 2024; 38(5): 4223–4237
https://doi.org/10.23812/j.biol.regul.homeost.agents.20243805.335

FTO-Mediated Downregulation of RAMP2-AS1 Promotes Glycolysis in Non-Small Cell Lung Cancer Cells by Inhibiting KLF9-Mediated Transcriptional Activation of LATS2

Yihui Fu[1,2], Yamei Zheng[2], Liang Li[3], Zhao Li[2], Jiwei Li[2], Shengming Liu[1,*]

[1]Department of Pulmonary and Critical Care Medicine, The First Affiliated Hospital of Jinan University, 510630 Guangzhou, Guangdong, China
[2]Department of Pulmonary and Critical Care Medicine, Hainan General Hospital (Hainan Affiliated Hospital of Hainan Medical University), 570301 Haikou, Hainan, China
[3]Department of Thoracic Surgery, Hainan General Hospital (Hainan Affiliated Hospital of Hainan Medical University), 570301 Haikou, Hainan, China
*Correspondence: tlsm@jnu.edu.cn (Shengming Liu)
Published: 1 May 2024

Background: Non-small cell lung cancer (NSCLC) is the most commonly occurring type of lung cancer. Previous studies have shown reduced expression of long noncoding RNA (lncRNA) RAMP2 antisense RNA1 (*RAMP2-AS1*) in NSCLC; however, the mechanism of *RAMP2-AS1* in NSCLC is not clear.

Methods: Cell Counting Kit-8 was used to assess cell viability. Cell apoptosis was detected using flow cytometry. Western blot assay was used to examine protein levels. N6-methyladenosine (m^6A)-RNA immunoprecipitation and Fluorescence *in situ* hybridization assays were used to detect the m^6A modification and cellular location of *RAMP2-AS1*, respectively. Glycolysis level was examined by commercial kits.

Results: *RAMP2-AS1* and large tumor suppressor 2 (*LATS2*) were downregulated in NSCLC tissues. Knockdown of fat mass and obesity-associated protein (*FTO*) elevated the m^6A modification *RAMP2-AS1*. Overexpression of *RAMP2-AS1* inhibited proliferation, glycolysis (indicated by high levels of glycolysis-related proteins, glucose consumption, lactate production, adenosine triphosphate content, and extracellular acidification rate) and induced cell apoptosis through Hippo signaling. *RAMP2-AS1* transcriptionally activated *LATS2* by binding with Krüppel-like factor 9 (KLF9). Downregulation of *LATS2* reversed the suppressive impact of *RAMP2-AS1* on cell glycolysis.

Conclusion: FTO-mediated m^6A demethylation of *RAMP2-AS1* increased glycolysis by reducing the impact of KLF9 on *LATS2* transcriptional activity. This study provides insights for developing novel therapeutic strategies for NSCLC.

Keywords: *RAMP2-AS1*; *FTO*; KLF9; *LATS2*; NSCLC

Introduction

Lung cancer is the second most common type of malignant tumor [1]. Non-small cell lung cancer (NSCLC) accounts for over 80% of all newly diagnosed cases of lung cancer [2]. Despite considerable advances in the understanding of lung cancer, it continues to be a major cause of cancer-associated mortality [3]. The poor prognosis of NSCLC is largely attributable to its high propensity for metastasis and recurrence. Notably, glycolysis plays a key role in inducing the growth and malignant behavior of NSCLC [4,5]. Exploring molecular targets to inhibit glycolysis in NSCLC may be an effective therapeutic direction.

Long noncoding RNAs (lncRNAs, >200 nt) are noncoding RNA transcripts [6]. LncRNAs play a key mediating role in carcinogenesis [7,8]. For instance, Wang Q *et al.* [9] found that upregulation of lncRNA *BBOX1-AS1* may enhance the sensitivity of colorectal cancer to radiotherapy through stabilization and activation of PFK1. In the study by Zhao *et al.* [10], lncRNA *AGAP2-AS1* was found to aggravate bladder cancer progression via interacting with N6-methyladenosine (m^6A) binding protein Insulin-like growth factor 2 mRNA binding protein 2 (IGF2BP2) to modulate mRNA stability of *LRG1*. Moreover, lncRNA RAMP2 antisense RNA1 (*RAMP2-AS1*) is a mediator in chondrosarcoma and breast cancer [11,12]. In addition, analysis of data from the Gene Expression Profiling Interactive Analysis (GEPIA) database showed downregulation of *RAMP2-AS1* in lung adenocarcinoma (LUAD) and lung squamous cell carcinoma (LUSC). Nevertheless, the mechanisms of *RAMP2-AS1* in NSCLC remain largely unknown.

Krüppel-like factors (KLFs) are DNA-binding factors with a wide range of functions [13,14]. Previous studies have indicated the involvement of KLFs, such as Krüppel-like factor 6 (KLF6) and Krüppel-like factor 2 (KLF2), in

Journal of
BIOLOGICAL REGULATORS
and Homeostatic Agents

the progression of NSCLC [15,16]. Krüppel-like factor 9 (KLF9) was considered as a tumor suppressor in hepatocellular carcinoma and renal cell carcinoma [17,18]. Using the RPISeq database, it was predicted that *RAMP2-AS1* has binding sites with KLF9; however, the relation between *RAMP2-AS1* and KLF9 in NSCLC remains unknown. Whether *RAMP2-AS1* affects NSCLC progression through binding with KLF9 deserves further exploration.

Large tumor suppressor 2 (LATS2) is a major serine/threonine kinase of the Hippo signaling, and it is located in chromosome 13Q1.11 [19]. LATS2 can regulate cell cycle by modulating YES-associated protein (YAP) and Tafazzin (TAZ) phosphorylation, which are crucial downstream mediators of Hippo signaling [20]. LATS2 is a modulator of mitotic progression which can activate the downstream proteins, inhibiting the growth of tumor cells [21]. LATS2 was demonstrated to promote death of NSCLC cells [22]. Additionally, prediction of JASPAR database suggested that KLF9 had binding sites with LATS2 promoter. Thus, *RAMP2-AS1* may regulate the progression of NSCLC by modulating KLF9 to regulate LATS2-mediated Hippo signaling. Further research is required to ascertain this hypothesis.

M^6A modification is a ubiquitous form of epitranscriptomic modification [23]. The m^6A modification process is modulated by multiple proteins, such as methyltransferases, related m^6A-binding proteins, and demethylases [24,25]. Study has suggested a modulatory role of m^6A modification in NSCLC [24]. Further, *RAMP2-AS1* was predicted to have multiple m^6A modification sites; however, whether *RAMP2-AS1* is regulated by m^6A modification remains unclear.

Therefore, the objective of this study was to investigate whether m^6A modification-mediated downregulation of *RAMP2-AS1* inhibits KLF9-mediated transcriptional activation of *LATS2*, thereby upregulating glycolysis in NSCLC cells and promoting tumor growth. Our findings may provide insights for developing a novel therapeutic strategy for NSCLC.

Material and Methods

Sample Collection

Twenty-four pairs of surgically resected NSCLC and adjacent tissue specimens were sourced from patients treated at Hainan General Hospital (Hainan Affiliated Hospital of Hainan Medical University). The tissues were stored at –80 °C. None of the patients had received specific drug treatment before tissue collection. According to the previous study [26], all clinicopathological diagnoses were confirmed by two experienced pathologists according to the eighth edition of the American Joint Commission on Cancer and the Union for International Cancer Control. Written informed consent was obtained from all patients. The research was approved by Hainan General Hospital (Hainan Affiliated Hospital of Hainan Medical University). The clinical study was conducted in accordance with the Declaration of Helsinki.

Cell Culture

H460 (cat. no. TCHu205), PC-9 (cat. no. SCSP-5085), H1975 (cat. no. TCHu193), A549 (cat. no. SCSP-503), H1299 (cat. no. SCSP-589) cells, and BEAS-2B (cat. no. GNHu27) cell lines were obtained from the Chinese Academy of Sciences (Beijing, China). Cells used in this study were authenticated by STR and no cross-contamination between cells was confirmed through mycoplasma testing. Cells were cultured as previously reported [27]. In brief, cells were seeded in RPMI-1640 medium (11875119, GIBCO, Grand Island, NY, USA) containing FBS (10%, A5669701, GIBCO, Grand Island, NY, USA) and 100 U/mL penicillin in conditions of 5% CO_2 and 37 °C.

Cell Transfection

NSCLC cells (5×10^3) were transfected with fat mass and obesity-associated protein (FTO) short hairpin RNA (shRNA) (sh-*FTO*: 5′-CGGTTCACAACCTCGGTTTAG-3′, C02007), short hairpin RNA of alkylation repair homolog protein 5 (sh-*ALKBH5*: 5′-GCTGCAAGTTCCAGTTCAAGC-3′, C02007), short hairpin RNA of large tumor suppressor 2 (sh-*LATS2*: 5′-CAGGACCAAACAGTGACACTT-3′, C02007), pcDNA3.1-*KLF9* (overexpression of KLF9 (oe-KLF9), C05008) or negative control (NC); short hairpin RNA of negtive control (sh-NC) and pcDNA3.1 via Lipofectamine 2000 (11668500, Invitrogen, Carlsbad, CA, USA) for 48 h, as previously described [28]. All plasmids were obtained from Genepharma (Pudong New Area, Shanghai, China).

For *RAMP2-AS1* overexpression, the overexpression of *RAMP2-AS1* (oe-RAMP2-AS1) vector was packaged into lentiviruses. For generating lentivirus-transduced lines, a virus was applied for infecting the cells. After incubation for 48 h, puromycin (2.5 μg/mL) was applied for 24 h to select the cells, as described elsewhere [29]. The transfection efficiency of oe-RAMP2-AS1 was confirmed by reverse transcription-quantitative polymerase chain reaction (RT-qPCR).

Cell Counting Kit-8 (CCK-8) Assay

CCK-8 assay was performed as previously described [30]. In brief, cells (5×10^3 per well) were seeded overnight in 96-well plates. After 48 h of treatment, CCK-8 (10 μL, CA1210, solarbio, Beijing, China) was added to each well for 2 h. Cell absorbance was measured at 450 nm using a microplate reader (VLBLATGD2, Thermo Fisher Scientific, Waltham, MA, USA).

Cell Apoptosis Analysis

Cell apoptosis was assessed using Annexin V-Fluorescein Isothiocyanate (FITC)/propidium iodide staining (C1062S, Shanghai, Beyotime, China) as previously reported [31]. Briefly, NSCLC cells were trypsinized and resuspended for 10 min. Then, 5 µL FITC and 5 µL Propidium (PI, 556463, BD Biosciences, Franklin Lake, NJ, USA) were applied for staining the cells in the dark for 15 min. Cell apoptosis was analyzed using flow cytometry, and then the cell apoptosis rate was calculated.

Bromodeoxyuridine (BrdU) Assay

Cells (1×10^4 per well) were plated and incubated overnight at 37 °C. BrdU cell proliferation was performed as previously reported [32]. Briefly, cells were exposed to 10 µL BrdU solution (B23151, Invitrogen, Carlsbad, CA, USA) for 30 min. The absorbance at 450 nm was measured. All experiments were performed in triplicate.

Reverse Transcription-Quantitative Polymerase Chain Reaction (RT-qPCR)

The detailed procedure for RT-qPCR was described as previously reported [33]. In brief, total RNA was extracted using TRIZOL reagent (15596018CN, Invitrogen, Carlsbad, CA, USA) and reverse-transcribed to synthesize cDNA using the reverse transcription kit (RR037Q, TaKaRa, Tokyo, Japan). Quantitative PCR was performed using a SYBR Primescript RT-qPCR kit (A46110, Applied Biosystems™, Foster City, CA, USA) on the ABI 7500 real-time PCR system (7500, Applied Biosystems, Foster City, CA, USA). qPCRs were applied as follows: 94 °C for 2 minutes, followed by 35 cycles (94 °C for 30 s and 55 °C for 45 s). The primers are shown below:

RAMP2-AS1: F, 5′-TGAGAAGTCAGGTGTGCG TA-3′ and R, 5′-AGAGACTTCTTCCAGGCAAC-3′. *LATS2*: F, 5′-ACAAGATGGGCTTCATCCAC-3′ and R, 5′-CTCCATGCTGTCCTGTCTGA-3′. *FTO*: F, 5′-ATTG GTAATCCAGGCTGCAC-3′ and R, 5′-GCAGCAAGTT CTTCCAAAGC-3′. *KLF9*: F, 5′-AACACGCCTCCGAA AAGAGG-3′ and R, 5′-TCGTCTGAGCGGGAGAACTT -3′. *ALKBH5*: F, 5′-AAGCGCAAGTATCAGGAGGA-3 ′ and R, 5′-TCGTTGTACAGGCCCTTCTC-3′. *β-actin*: F, 5′-AGCGAGCATCCCCCAAAGTT-3′ and R, 5′-GGG CACGAAGGCTCATCATT-3′. The $2^{-\Delta\Delta Ct}$ method was applied for calculating the relative expressions normalized to *β-actin* expression.

Western Blot

Western blot was performed according to a previous study [34]. Briefly, RIPA buffer was applied for protein isolation, and the BCA kit was applied for quantification. SDS-PAGE (10%) was used for separating the proteins, and then the proteins were transferred to PVDF membranes (ISEQ07850, Millipore, Boston, MA, USA). The membranes were then incubated overnight with primary antibodies at 4 °C after blocking, followed by incubation with secondary anti-rabbit antibody (1:5000, ab7090, Abcam, Cambridge, UK) for 1 h. Odyssey Imaging System was applied for scanning the membranes, and analysis was performed using Odyssey v2.0 software (version 2, Genecompany, Beijing, China). The primary antibodies were as follows: anti-LATS2 (1:1000, PA5-120433, Thermo Fisher Scientific, Waltham, MA, USA), anti-FTO (1:1000, 27226-1-AP, Proteintech, Chicago, IL, USA), anti-ALKBH5 (1:1000, ab195377, Abcam, Cambridge, UK), anti-KLF9 (1:1000, ab227920, Abcam, Cambridge, UK), anti-pyruvate kinase M2 (PKM2) (1:1000, 4053S, Cell Signaling Technology, Boston, MA, USA), anti-Lactate dehydrogenase A (LDHA) (1:1000, 19987-1-AP, Proteintech, Chicago, IL, USA), anti-hexokinase 2 (HK2) (1:1000, ab209847, Abcam, Cambridge, UK), anti-YAP1 (1:1000, ab205270, Abcam, Cambridge, UK), anti-phospho-YAP1 (p-YAP1) (1:1000, ab76252, Abcam, Cambridge, UK), anti-TAZ (1:1000, ab110239, Abcam, Cambridge, UK), anti-phospho-TAZ (p-TAZ) (1:1000, AF4316, Affinity, Changzhou, China), and anti-β-actin (1:1000, ab8227, Abcam, Cambridge, UK).

Glucose Consumption and Lactate Production

Glucose consumption and lactate production were measured as previously described [35]. For the glucose consumption assay, cells were cultured with a complete medium for 1 day. After removal of the complete medium, cells were cultured with low glucose medium for 4 h. Glucose Uptake Assay Kit (MAK083, Sigma Aldrich, Saint Louis, MO, USA) was applied to measure the ability of cells to take up glucose. For the lactate production assay, the culture medium was replaced with a fresh medium. After incubation for 6 h, the lactate content was measured using the Colorimetric L-Lactate Assay Kit (ab65331, Abcam, Cambridge, UK).

Adenosine Triphosphate (ATP) Content Detection

ATP content was detected using the ATP assay kit (S0026, Beyotime, Shanghai, China) as previously reported [36]. ATP determination buffer (100 µL) was applied for ATP extraction. Cells (5×10^6) were centrifuged at 12,000 rpm for 5 min. Next, supernatants were utilized for measuring ATP. After the reaction mixture was incubated for 30 min avoiding light, the samples were tested using a microplate reader at 570 nm.

Examination of Extracellular Acidification Rate (ECAR)

The ECAR was measured on an XF96 Extracellular Flux analyzer (XF96, Seahorse Bioscience, Boston, MA, USA) as previously reported [37]. Cells were seeded in the XF-96 microwell plates (101085-004, Seahorse Bioscience, Boston, MA, USA). After measurement of the basic acidification rate, 10 mM glucose was added, and then glycoly-

Journal of
BIOLOGICAL REGULATORS
and Homeostatic Agents

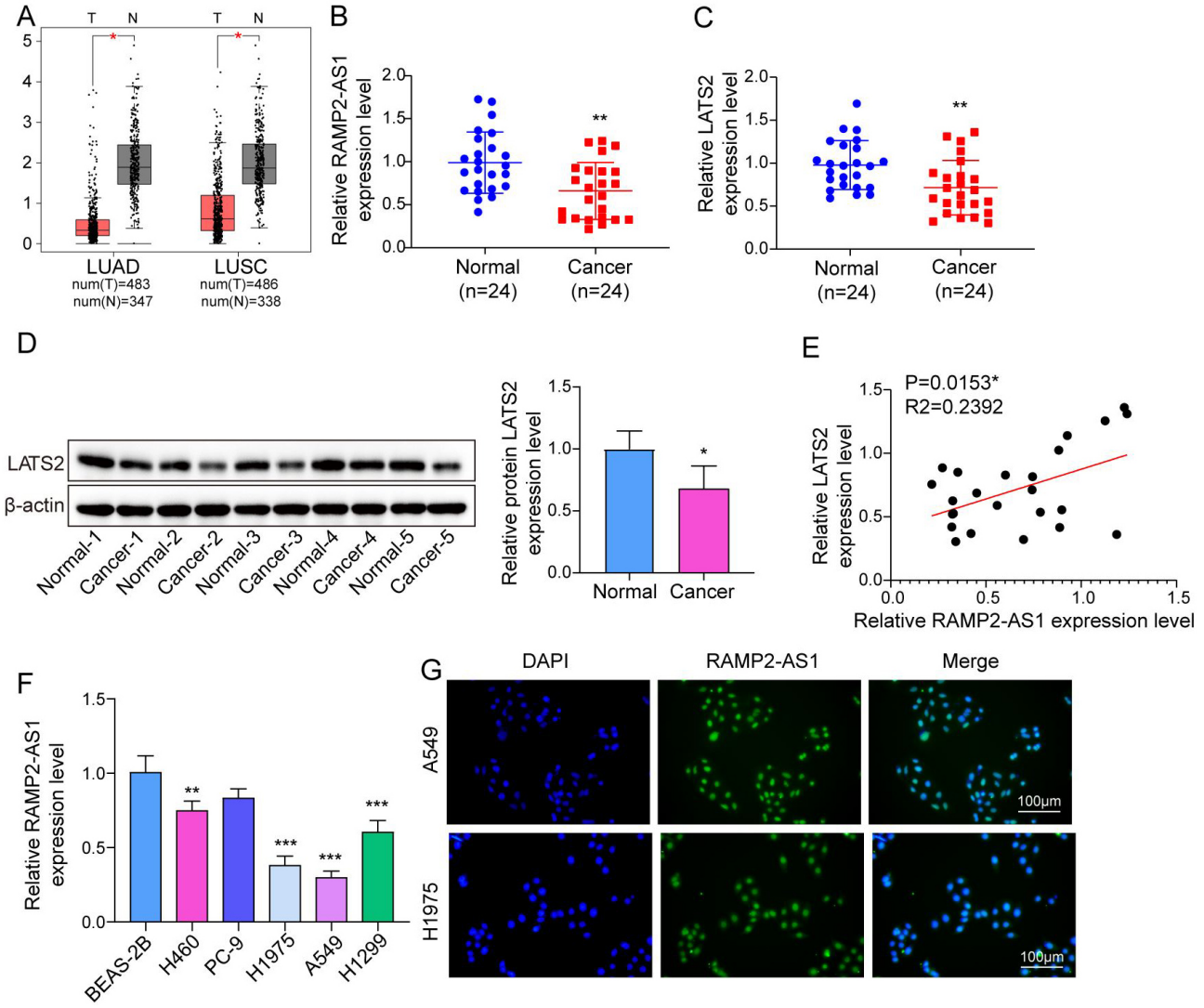

Fig. 1. *RAMP2-AS1* was downregulated in NSCLC. (A) Quantitative analysis of *RAMP2-AS1* level in NSCLC and adjacent normal tissues based on GEPIA database. T, tumor; N, normal. (B) *RAMP2-AS1* level assessed by RT-qPCR (n = 24 per group). (C) Large tumor suppressor 2 (*LATS2*) level examined by RT-qPCR (n = 24 per group). (D) LATS2 level in NSCLC determined by Western blot assay (n = 5 per group). (E) Correlation between *RAMP2-AS1* and *LATS2* assessed using Pearson's correlation analysis. (F) *RAMP2-AS1* expression in BEAS-2B and NSCLC cells determined by RT-qPCR (n = 3 per group). (G) Fluorescence *in situ* hybridization (FISH) assay showing the cellular location of *RAMP2-AS1* in NSCLC. All data were obtained from at least three replicate experiments. *$p < 0.05$, **$p < 0.01$, ***$p < 0.001$. GEPIA, Gene Expression Profiling Interactive Analysis; RT-qPCR, reverse transcription-quantitative polymerase chain reaction; *RAMP2-AS1*, RAMP2 antisense RNA1; LUAD, lung adenocarcinoma; LUSC, lung squamous cell carcinoma; DAPI, 4′,6-diamidino-2-phenylindole; NSCLC, non-small cell lung cancer.

sis was detected. Next, to measure the maximum glycolysis ability, oligomycin was added to inhibit oxidative phosphorylation. All reagents were added at 0 min and the incubation temperature was maintained at 38.5 °C. Cells were detected every 7 min following continuous administration of 10 mM glucose and inhibitors (1 μM oligomycin and 50 mM 2-Deoxy-D-arabino-hexose (2-DG)).

M^{6}A-RNA Immunoprecipitation (MeRIP)

MeRIP assay was performed as previously reported [38]. Briefly, RNA (1 μg) was extracted using the TRIZOL reagent (15596018CN, Invitrogen, Carlsbad, CA, USA). Subsequently, mRNA was immunoprecipitated with Protein A beads (80103G, Invitrogen, Carlsbad, CA, USA) and anti-m^{6}A antibody (ab208577, Abcam, Cambridge, UK) after fragmentation. The immunoprecipitated RNA was eluted for the construction of the m^{6}A MeRIP library. Then, the PrimeScript Kit was used for cDNA synthesis. *RAMP2-AS1* level was determined by RT-qPCR using the SYBR-Green and StepOnePlus system (A46110, Applied Biosystems™, Foster City, CA, USA).

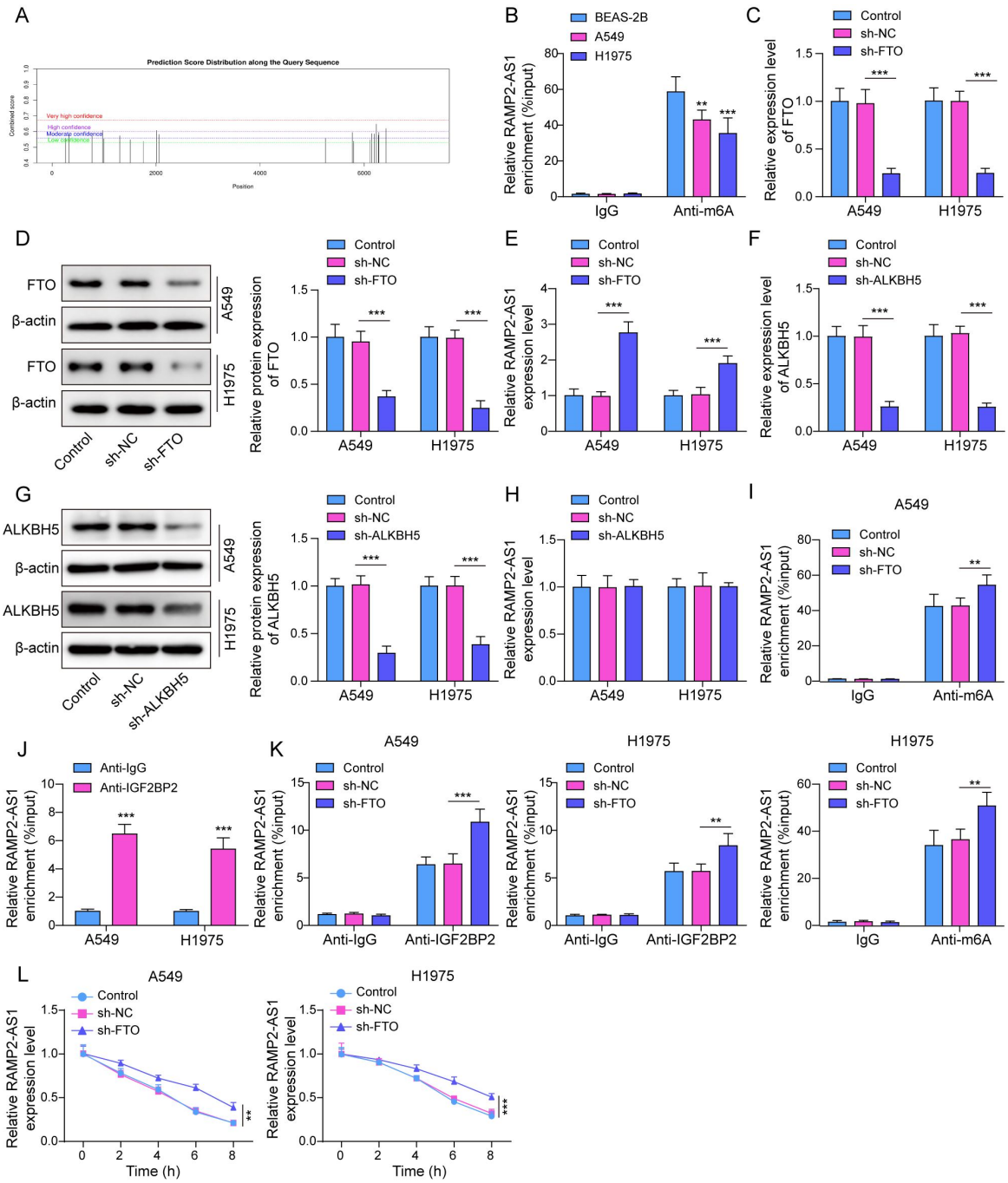

Fig. 2. FTO mediated-m^{6}A demethylation of *RAMP2-AS1* inhibited *RAMP2-AS1* expression. (A) N6-methyladenosine (m^{6}A) modification of *RAMP2-AS1* predicted by SRAMP database; (B) Results of MeRIP assay showing the m^{6}A modification level of *RAMP2-AS1*. NSCLC cells were exposed to sh-FTO. (C,D) Quantitative analysis of RT-qPCR and Western blot results showing the transfection efficiency; (E) The level of *RAMP2-AS1* assessed by RT-qPCR. NSCLC cells were exposed to sh-alkylation repair homolog protein 5 (ALKBH5). (F,G) Results of RT-qPCR and Western blot assay for determining ALKBH5 level; (H) *RAMP2-AS1* level determined by RT-qPCR; (I) RT-qPCR results showing the m^{6}A modification level of *RAMP2-AS1* in NSCLC cells transfected with sh-FTO. (J) RIP assay for testing the binding between *RAMP2-AS1* and Insulin-like growth factor 2 mRNA binding protein 2 (IGF2BP2). NSCLC cells were transfected with sh-FTO. (K) RIP assay for testing the binding between *RAMP2-AS1* and IGF2BP2. (L) Results of RNA stabilization assay to determine the half-life of *RAMP2-AS1* mRNA. n = 3 per group. All data were obtained from at least three replicate experiments. $^{**}p < 0.01$, $^{***}p < 0.001$. SRAMP, Sequence-based RNA adenosine methylation site predictor; MeRIP, M^{6}A-RNA immunoprecipitation; RIP, RNA Immunoprecipitation; shRNA, short hairpin RNA; FTO, fat mass and obesity-associated protein; sh-FTO, short hairpin RNA of fat mass and obesity-associated protein; sh-NC, short hairpin RNA of negtive control; sh-ALKBH5, short hairpin RNA of alkylation repair homolog protein 5; IgG, Immunoglobulin G.

Journal of
BIOLOGICAL REGULATORS
and Homeostatic Agents

Fluorescence in Situ Hybridization Assay

To explore the cellular location of *RAMP2-AS1*, a Fluorescence *in situ* hybridization (FISH) assay was performed as described elsewhere [39]. Specific probes for *RAMP2-AS1* were obtained from RiboBio (Guangzhou, Guangdong, China). The Ribo FISH kit was used for FISH experiments. Briefly, the experiments were applied after the attainment of 60% confluence. Prechilled permeate was used for cell permeation at 4 °C. Subsequently, 4% paraformaldehyde was applied for fixing the cells followed by 0.5% Triton. The fixed cells were incubated with Probe Mix stock solution. The images were captured using a fluorescence microscope.

RNA Immunoprecipitation (RIP) Assay

To detect the binding among *RAMP2-AS1* and IGF2BP2/KLF9, RIP assay was performed as previously described [40]. RIPA lysis buffer was applied for lysing the cells for 10 min at 4 °C, and then the cells were centrifuged for 5 min at 200 g for cell lysate collection. The cell lysate was incubated with IGF2BP2/KLF9 antibody-labeled A + G magnetic beads for 16 h at 4 °C. Immunoglobulin G (IgG) served as a NC. In addition, "Input" was obtained from the harvested supernatant which was regarded as control. For RNA isolation, Proteinase K buffer (150 µL) was applied to detach the isolated immunoprecipitated complex. RT-qPCR was employed to assess the relative expression level.

RNA Stability Assay

RNA stability assay was performed as previously reported [41]. In brief, cells (0.8×10^5/well) were incubated with actinomycin D (5 µg/mL, 50-76-0, Sigma Aldrich, Saint Louis, MO, USA) for 2, 4, 6, or 8 h. Isolated RNA was quantified after actinomycin D treatment, and then the level of *RAMP2-AS1* was tested using RT-qPCR.

Chromatin Immunoprecipitation (ChIP)

The binding relation among KLF9 and *LATS2* promoter was investigated using ChIP assay as previously reported [42]. In brief, ChIP Kit (abs50034, Absin, Shanghai, China) was applied for ChIP assays. Cells were incubated with 1% formaldehyde (P1111, Solarbio, Beijing, China) for cross-link generation of DNA protein. Cell lysates were sonicated to yield genomic DNA fragments (200–600 bp). The isolated chromatin was used for immunoprecipitation with specific antibodies (anti-KLF9, ab227920, Abcam, Cambridge, UK). IgG served as a negative control.

RNA-Pull Down Assay

RNA-pull down assay was applied to confirm the interaction among *RAMP2-AS1* and KLF9 as previously reported [43]. Briefly, biotinylated NC or *RAMP2-AS1* was cultured with cell lysates for 2 h. Then, immunomagnetic beads (streptavidin-labeled) were applied to capture the *RAMP2-AS1*/KLF9 complex for 1 h. Buffer containing Proteinase K was applied for incubating the complexes for 1 h. The proteins in the RNA-protein complex in the pull-down assays were identified by Western blot assay.

In Vivo Study

BALB/c nude mice (n = 15) were obtained from Vital River and housed in specific pathogen-free conditions. A549 cells with stable overexpression of *RAMP2-AS1* were subcutaneously transplanted in unilateral underarm of mice as previously reported [44]. BALB/C nude mice were administered subcutaneous injection of 0.1 mL PBS containing 2×10^6 A549 cells with stable overexpression of *RAMP2-AS1*. The tumor volume was calculated using the following formula: $V = l\,w^2/2$ (l: length, w: width). The tumor volume was investigated every 5 days. After 25 days of oe-RAMP2-AS1 treated A549 cell treatment, nude mice were euthanized using excess carbon dioxide, and tumors were harvested and weighed. Antigen identified by monoclonal antibody Ki-67 (Ki67) and LATS2 expressions in tumor tissues were assessed by Immunohistochemistry (IHC) staining. All animal procedures were in accordance with National Institutes of Health guidelines and approved by the Animal Care and Use Committee of Hainan General Hospital (Hainan Affiliated Hospital of Hainan Medical University).

IHC Staining

The detailed procedure for IHC staining is described elsewhere [45]. Briefly, the tumor tissues were fixed overnight with paraformaldehyde (4%). Next, tissues were paraffin-embedded and cut into sections (5-µm-thick). Sections were rehydrated after deparaffinization. For antigen retrieval, sections were heated in sodium citrate buffer. Then, the sections were incubated with H_2O_2 (3%) for 25 min, followed by incubation with goat serum for 30 min after blocking. Then, the samples were incubated overnight with primary antibodies (anti-Ki67, 1:500, ab15580, Abcam, Cambridge, UK; anti-LATS2, 1:100, PA5-120433, Thermo Fisher Scientific, Waltham, MA, USA) at 4 °C, followed by incubation with secondary antibody (HRP-labeled) at 37 °C for 30 min. Finally, freshly prepared DAB was used for developing the color. The images were captured using a light microscope.

Bioinformatics Analysis

The expression of *RAMP2-AS1* in LUAD and LUSC was predicted using the GEPIA (http://gepia.cancer-pku.cn/) database [46]. The binding sites of the *LATS2* promoter and KLF9 were predicted by JASPAR (http://jaspar.genereg.net/) database [47]. The m^6A modification site of *RAMP2-AS1* was predicted by the Sequence-based RNA adenosine methylation site predictor (SRAMP) (http://www.cuilab.cn/sramp) database [48].

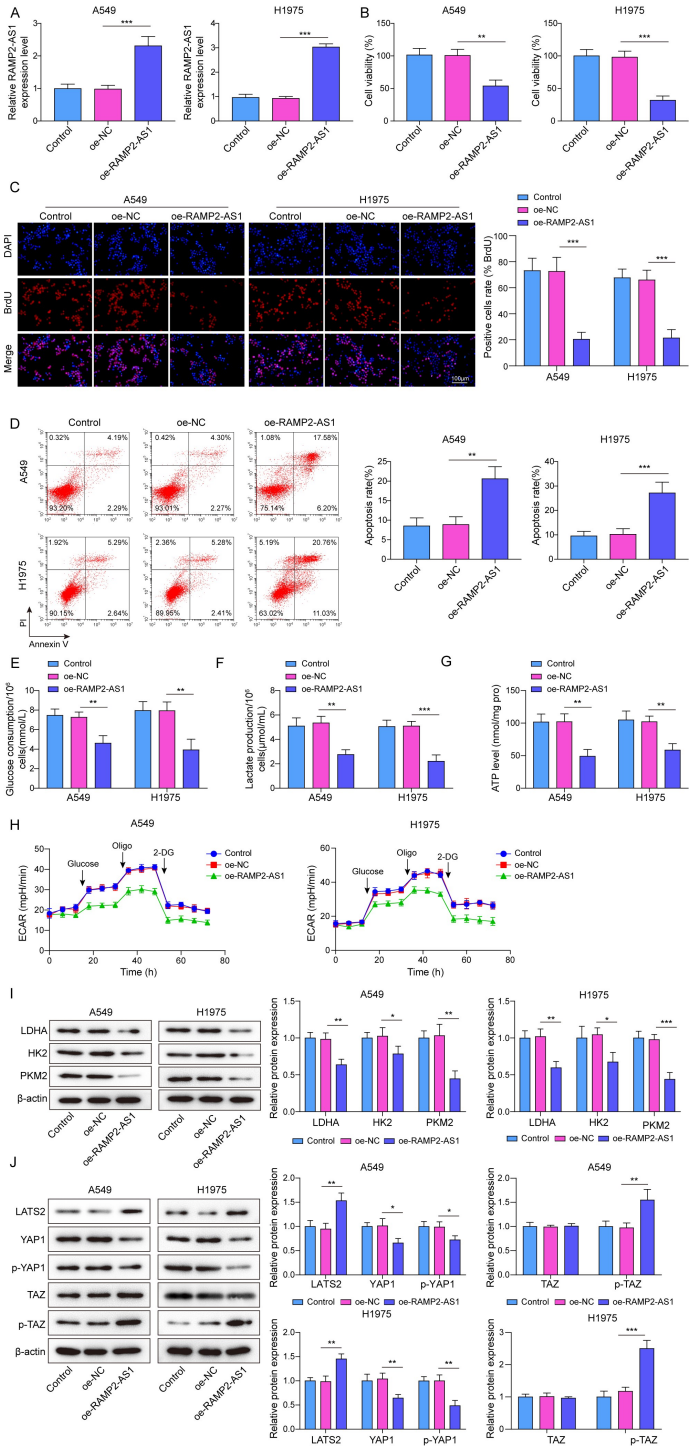

Fig. 3. *RAMP2-AS1* inhibited glycolysis in NSCLC cells through mediation of Hippo signaling. NSCLC cells were overexpressed with oe-RAMP2-AS1. (A) Quantitative analysis of *RAMP2-AS1* level determined by RT-qPCR. (B) NSCLC cell viability assessed by CCK-8 assay. (C) NSCLC cell proliferation tested using BrdU assay. (D) Results of flow cytometry for detecting cell apoptosis. (E) Glucose consumption assessed using commercial kits. (F) Lactate production assessed using commercial kits. (G) ATP content examined using commercial kits. (H) The ECAR in NSCLC cells determined using commercial kits. (I,J) Western blot showing the protein expressions of PKM2, LDHA, TAZ, p-TAZ, YAP1, p-YAP1, LATS2, and HK2 levels in NSCLC cells. n = 3 per group. All data were obtained from at least three replicate experiments. $*p < 0.05$, $**p < 0.01$, $***p < 0.001$. PKM2, pyruvate kinase M2; LDHA, Lactate dehydrogenase A; TAZ, Tafazzin; p-TAZ, phospho-TAZ; YAP1, YES-associated protein 1; p-YAP1, phospho-YAP1, HK2, hexokinase 2; CCK-8, Cell Counting Kit-8; BrdU, Bromodeoxyuridine; ATP, adenosine triphosphate; ECAR, Extracellular acidification rate; oe-NC, negative control of overexpression; oe-RAMP2-AS1, overexpression of *RAMP2-AS1*.

Journal of
BIOLOGICAL REGULATORS
and Homeostatic Agents

Statistical Analysis

Statistical analysis was performed as previously reported [49]. All experiments were conducted in triplicate and mean ± standard deviation (SD) values were used for the analysis. One-way analysis of variance followed by Tukey's test was applied for multi-group comparisons. Differences between two groups were assessed for statistical significance using the student's *t*-test. All analysis was performed using GraphPad Prism software (version 8, GraphPad Software, San Diego, CA, USA). $p < 0.05$ was considered indicative of statistical significance.

Results

RAMP2-AS1 was Downregulated in NSCLC Tissues and Cells

LncRNA *RAMP2-AS1* is identified as a tumor suppressor gene in several human malignant tumors [12,50]. However, the role of *RAMP2-AS1* in NSCLC remains unclear. To detect the role of *RAMP2-AS1* in NSCLC, the GEPIA database was used to predict the *RAMP2-AS1* levels. *RAMP2-AS1* levels in LUAD and LUSC tissues were markedly lower than those in normal tissues (Fig. 1A). RT-qPCR demonstrated lower expression of *RAMP2-AS1* in NSCLC tissues compared with para-carcinoma tissues (Fig. 1B). Analogously, NSCLC tissues showed low expression of LATS2 (Fig. 1C,D). Moreover, the *RAMP2-AS1* level was positively correlated with *LATS2* in NSCLC (Fig. 1E). To further verify the expression of *RAMP2-AS1* in NSCLC, *in vitro* experiments were performed. The data revealed that the *RAMP2-AS1* level in NSCLC cells was much lower than in BEAS-2B cells (Fig. 1F). Since the level of *RAMP2-AS1* was altered more significantly in A549 and H1975 cells, these two cell lines were selected for subsequent analysis. Furthermore, *RAMP2-AS1* was mainly distributed in the NSCLC cell nucleus (Fig. 1G). In summary, *RAMP2-AS1* was poorly expressed in NSCLC.

FTO Mediated-M^{6}A Demethylation of RAMP2-AS1 Inhibited RAMP2-AS1 Expression

M^{6}A modification plays a vital role in cancer development [51,52]. Thus, we used the SRAMP database to predict the m^{6}A modification sites of *RAMP2-AS1*. As shown in Fig. 2A, there were multiple m^{6}A modification sites in *RAMP2-AS1*. The m^{6}A modification level of *RAMP2-AS1* was significantly downregulated in NSCLC cells (Fig. 2B). Since m^{6}A is regulated by methylases (such as METTL3) and demethylases (such as ALKBH5 and FTO) [53], and *RAMP2-AS1* m^{6}A was downregulated in NSCLC, it can be hypothesized that the *RAMP2-AS1* is regulated by m^{6}A demethylases. Then we explored whether *RAMP2-AS1* was mediated by demethylases FTO and ALKBH5. NSCLC cells were transfected with sh-FTO, and then the transfection efficiency was assessed using RT-qPCR and Western blot assays. The data showed that the level of FTO in NSCLC cells was significantly reduced by sh-FTO (Fig. 2C,D). In addition, FTO silencing elevated the level of *RAMP2-AS1* (Fig. 2E). Then, to explore the impact of ALKBH5 on *RAMP2-AS1* level, cells were transfected with sh-ALKBH5. As illustrated in Fig. 2F,G, the level of ALKBH5 was reduced by sh-ALKBH5. However, sh-ALKBH5 did not influence the *RAMP2-AS1* level in NSCLC cells (Fig. 2H). These results suggest that RAMP2-AS1 may be regulated by demethylases ALKBH5 rather than FTO in NSCLC cells. Moreover, the silencing of FTO led to a remarkable upregulation of the m^{6}A modification level of *RAMP2-AS1* (Fig. 2I). These results suggested that the m^{6}A modification of *RAMP2-AS1* was regulated by FTO. RIP assay revealed that *RAMP2-AS1* could bind with m^{6}A recognition protein IGF2BP2, and the phenomenon was further enhanced by sh-FTO (Fig. 2J,K). Furthermore, the downregulation of FTO led to a notable increase in the half-life of *RAMP2-AS1* mRNA (Fig. 2L). The above findings suggested that FTO may inhibit the level of *RAMP2-AS1* by suppressing the recognition of IGF2BP2 by m^{6}A-modified *RAMP2-AS1*.

Overexpression of RAMP2-AS1 Reduced Glycolysis in NSCLC Cells through Mediating Hippo Signaling

To detect the function of *RAMP2-AS1* in NSCLC, cells were overexpressed with oe-RAMP2-AS1. As shown in Fig. 3A, oe-RAMP2-AS1 increased the *RAMP2-AS1* level in NSCLC cells. Overexpression of *RAMP2-AS1* reduced tumor cell viability and proliferation and promoted apoptosis (Fig. 3B–D). Altered glycolysis is a biochemical fingerprint of cancer cells and is one of the "hallmarks of cancer" [54]. Overexpression of *RAMP2-AS1* led to a significant decline in lactate production and glucose consumption in NSCLC cells (Fig. 3E,F). Consistently, the upregulation of *RAMP2-AS1* significantly inhibited the production of ATP and ECAR in NSCLC cells (Fig. 3G,H). Overexpression of *RAMP2*-AS1 led to a marked downregulation of glycolysis-related protein (PKM2, LDHA, and HK2) levels (Fig. 3I). Moreover, *RAMP2-AS1* overexpression decreased the expression of Hippo signaling-related proteins p-YAP1 and YAP1 and increased the expression of Hippo signaling-associated proteins LATS2 and p-TAZ in NSCLC cells (Fig. 3J). Collectively, these findings suggest that overexpression of *RAMP2-AS1* inhibited the glycolysis in NSCLC cells through mediation of Hippo signaling.

RAMP2-AS1 Promoted the Transcriptional Activation of LATS2 through Binding with KLF9

KLF9 is a transcriptional factor that is closely related to the progression of multiple human malignant tumors, including NSCLC [55,56]. For exploring the role of KLF9 in NSCLC, clinical samples were subjected to RT-qPCR analysis. The results showed significantly lower *KLF9* mRNA levels in NSCLC tissues compared to normal tissues (Fig. 4A). *KLF9* level showed a positive correlation

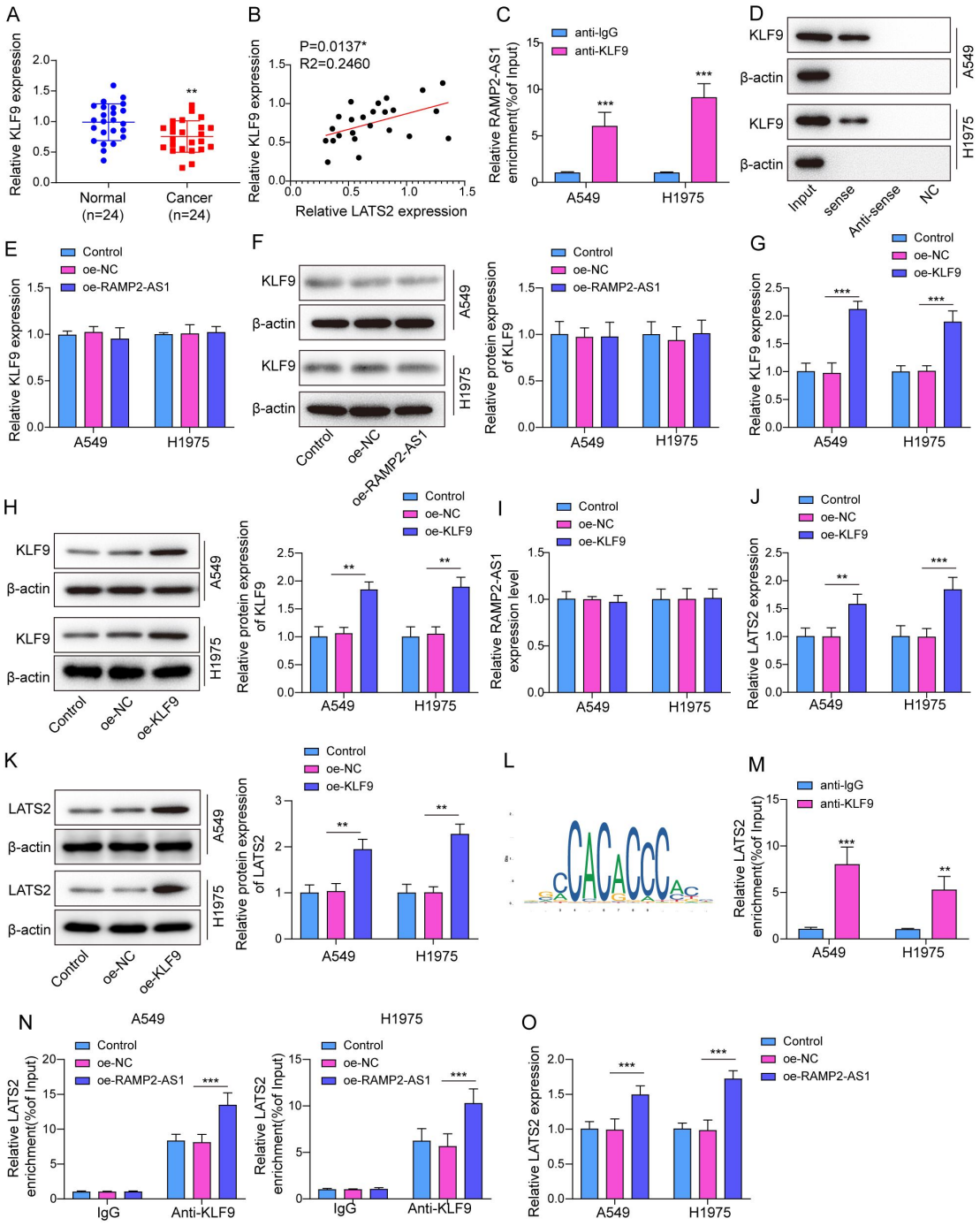

Fig. 4. *RAMP2-AS1* promoted the transcriptional activation of LATS2 through binding with KLF9. (A) RT-qPCR results showing the mRNA level of *KLF9* in NSCLC and adjacent normal tissues (n = 24 per group). (B) Correlation between KLF9 and LATS2 assessed using Pearson's correlation analysis. (C) RIP assay to examine binding between *RAMP2-AS1* and KLF9. (D) RNA pull-down assay to examine binding between *RAMP2-AS1* and KLF9. (E,F) Cells were overexpressed with oe-RAMP2-AS1. RAMP2-AS1 level was examined using RT-qPCR and Western blot assay. NSCLC cells were overexpressed with oe-KLF9. (G,H) RT-qPCR and Western blot assay to determine the transfection efficiency. (I) RT-qPCR results showing the level of *RAMP2-AS1*. (J,K) RT-qPCR and Western blot results showing LATS2 level. (L) Binding between KLF9 and LATS2 promoter was predicted using JASPAR. (M) Binding among KLF9 and LATS2 promoter was investigated using ChIP assay. NSCLC cells were overexpressed with RAMP2-AS1. (N) Binding among KLF9 and LATS2 promoter was investigated using ChIP assay. (O) *LATS2* level determined using RT-qPCR. n = 3 per group for *in vitro* study. All data were obtained from at least three replicate experiments. *$p < 0.05$, **$p < 0.01$, ***$p < 0.001$. KLF9, Krüppel-like factor 9; ChIP, Chromatin immunoprecipitation; oe-KLF9, overexpression of KLF9.

Journal of
BIOLOGICAL REGULATORS
and Homeostatic Agents

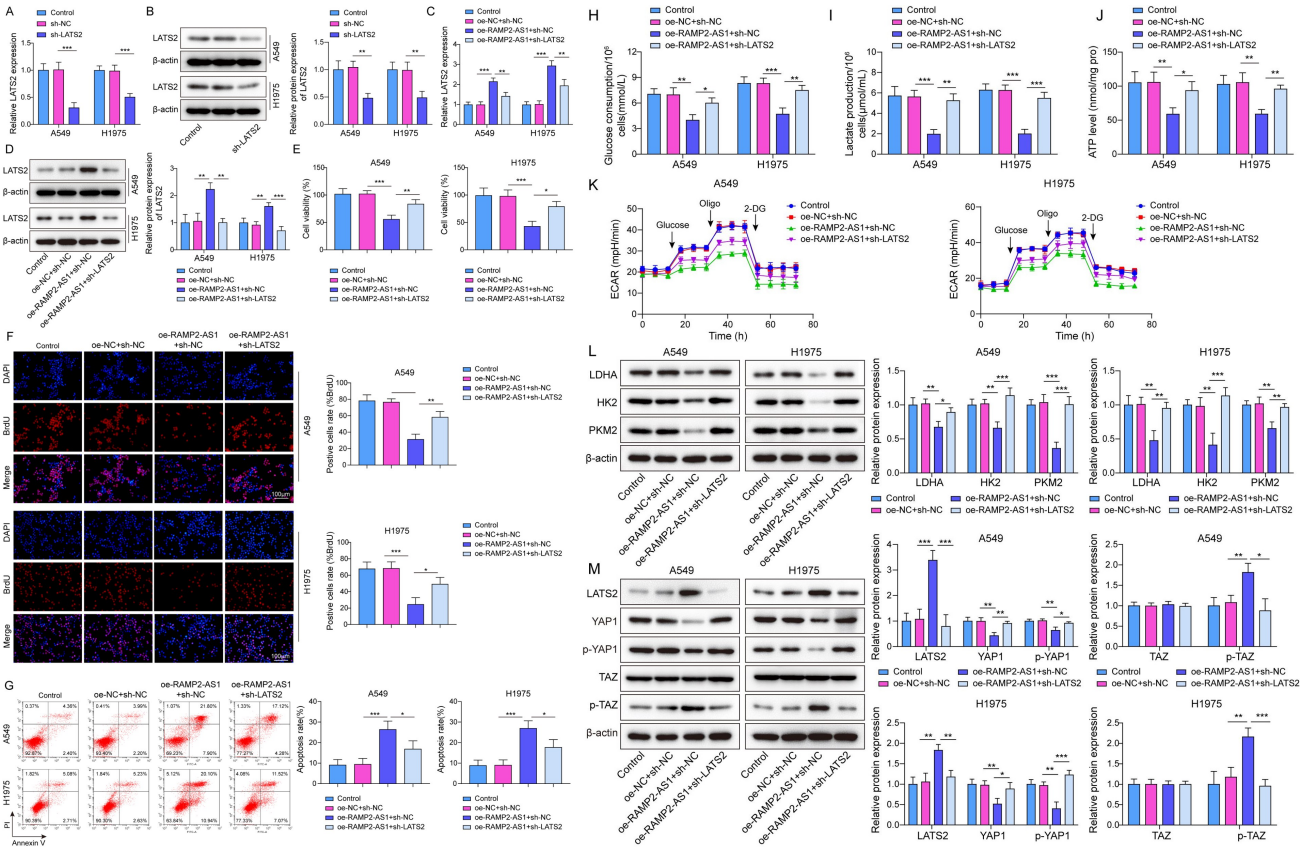

Fig. 5. Knockdown of LATS2 reversed *RAMP2-AS1* overexpression-induced inhibition of glycolysis in NSCLC cells. (A,B) RT-qPCR and Western blot results showing LATS2 level in cells exposed to sh-LATS2. NSCLC cells were overexpressed with oe-RAMP2-AS1 and then transfected with sh-LATS2. (C,D) LATS2 level in NSCLC cells examined through RT-qPCR and Western blot assay. (E) CCK-8 assay results showing the NSCLC cell viability. (F) Cell proliferation examined using BrdU assay. (G) Flow cytometry to detect cell apoptosis. (H) Glucose consumption assessed using commercial kits. (I) Lactate production determined using commercial kits. (J) ATP content assessed using commercial kits. (K) ECAR in NSCLC cells assessed using commercial kits. (L,M) Western blot showing the protein expressions of PKM2, LDHA, TAZ, p-TAZ, p-YAP1, YAP1, LATS2, and HK2 levels. n = 3 per group. All data were obtained from at least three replicate experiments. *$p < 0.05$, **$p < 0.01$, ***$p < 0.001$. sh-LATS2, short hairpin RNA of large tumor suppressor 2; 2-DG, 2-Deoxy-D-arabino-hexose.

with *LATS2* (Fig. 4B). Moreover, compared with the anti-IgG group, anti-KLF9 significantly enriched *RAMP2-AS1* (Fig. 4C). Furthermore, biotin-tagged *RAMP2-AS1* significantly enriched KLF9 protein, while the antisense *RAMP2-AS1* had no such effect (Fig. 4D). These results indicated that *RAMP2-AS1* could bind with KLF9. In addition, overexpression of *RAMP2-AS1* had a limited effect on KLF9 level (Fig. 4E,F). These data indicated that *RAMP2-AS1* did not affect the expression level of KLF9, but that it may only affect KLF9 function as a molecular scaffold. Next, cells were overexpressed with oe-KLF9. As expected, KLF9 level was elevated by oe-KLF9 (Fig. 4G,H). The level of *RAMP2-AS1* was not affected by the upregulation of KLF9, and this result demonstrated that KLF9 was not the transcriptional factor of *RAMP2-AS1* (Fig. 4I). However, oe-KLF9 significantly increased the expression of LATS2 (Fig. 4J,K). Using the JASPAR database, KLF9 was predicted to have binding sites with *LATS2* promoter (Fig. 4L). The result confirmed that KLF9 can bind with *the LATS2* promoter, and this binding was further increased by overexpression of *RAMP2-AS1* (Fig. 4M,N). Furthermore, upregulation of *RAMP2-AS1* significantly increased the expression of *LATS2* (Fig. 4O). These data indicated that *RAMP2-AS1* promoted the transcriptional activation of *LATS2* through binding with KLF9.

Knockdown of LATS2 Reversed RAMP2-AS1 Overexpression-Induced Inhibition of Glycolysis

To detect the role of LATS2 in *RAMP2-AS1*-mediated glycolysis of NSCLC cells, NSCLC cells were exposed to sh-LATS2. As demonstrated in Fig. 5A,B, sh-LATS2 inhibited the LATS2 level in NSCLC cells. Further, *RAMP2-AS1* overexpression-induced upregulation of LATS2 was abolished by sh-LATS2 (Fig. 5C,D). Consistently, silencing of LATS2 markedly rescued the impact of oe-RAMP2-AS1 on the viability, proliferation, and apopto-

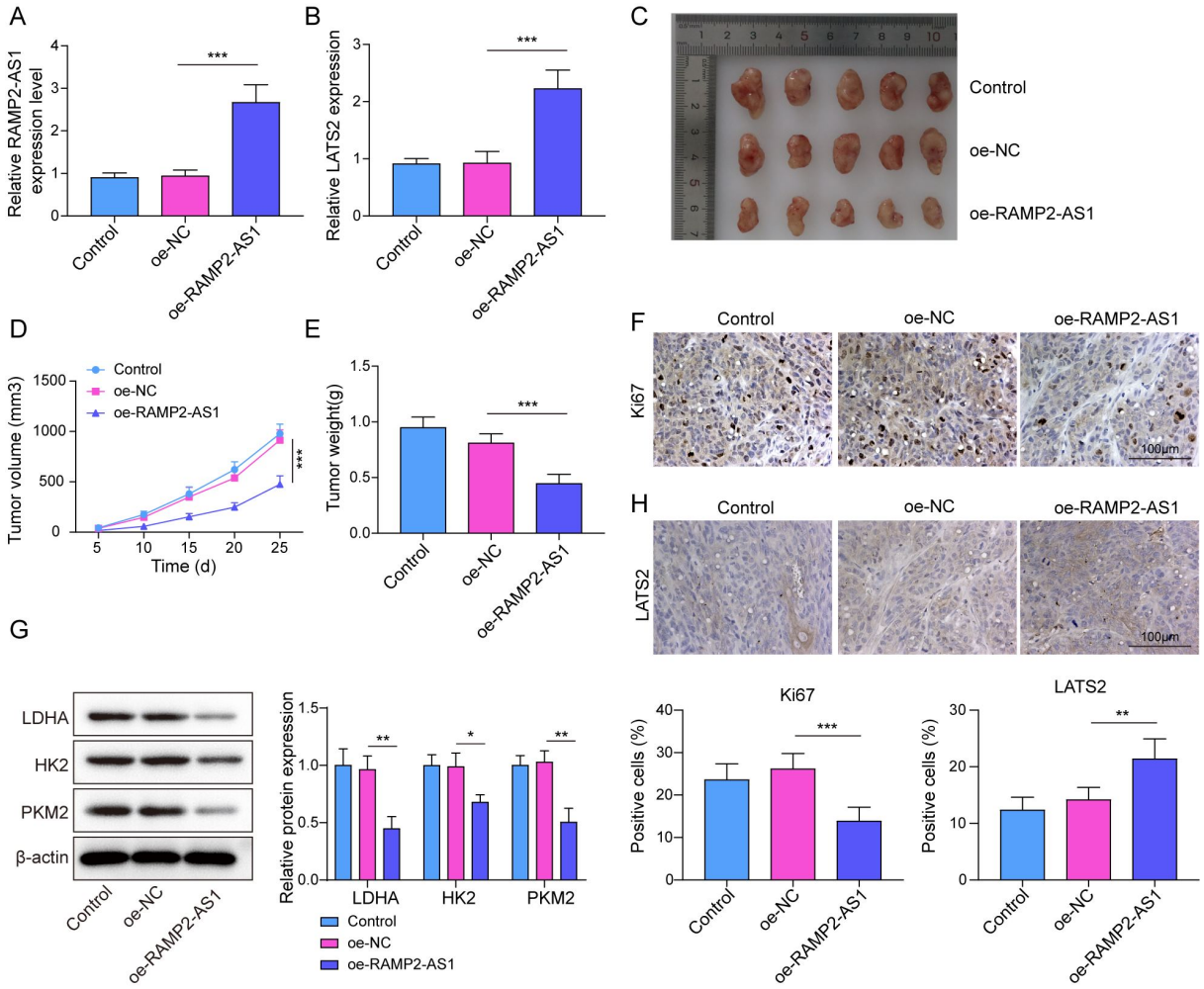

Fig. 6. *RAMP2-AS1* inhibited tumorigenesis and glycolysis in NSCLC *in vivo* through upregulation of LATS2. Mice were injected subcutaneously with A549 cells overexpressed with oe-NC or oe-RAMP2-AS1. (A,B) *RAMP2-AS1* and *LATS2* levels in mice examined using RT-qPCR (n = 3 per group). (C) Photographs of tumor tissues (n = 5 per group). (D) Analysis of tumor volume (n = 5 per group) and (E) tumor weight (n = 5 per group). (F) IHC staining to determine Ki-67 level (n = 5 per group). (G) Western blot showing the protein expressions of PKM2, LDHA, and HK2 levels in mice (n = 3 per group). (H) IHC staining to determine LATS2 level (n = 5 per group). $*p < 0.05$, $**p < 0.01$, $***p < 0.001$. IHC, Immunohistochemistry.

sis of NSCLC cells (Fig. 5E–G). Furthermore, the knockdown of LATS2 significantly reversed the oe-RAMP2-AS1-induced decline in glucose consumption, lactate production, ATP content, and ECAR (Fig. 5H–K). Moreover, silencing of LATS2 abolished the effect of oe-RAMP2-AS1 on glycolysis-associated proteins and Hippo-associated proteins (Fig. 5L,M). In summary, silencing of LATS2 reversed *RAMP2-AS1* overexpression-induced inhibition of glycolysis in NSCLC cells.

Overexpression of RAMP2-AS1 Inhibited Tumorigenesis and Glycolysis in NSCLC in Vivo through Upregulation of LATS2

We then established a xenograft mice model to confirm the impact of *RAMP2-AS1 in vivo*. As indicated in Fig. 6A,B, oe-RAMP2-AS1 significantly upregulated the levels of *RAMP2-AS1* and *LATS2* in NSCLC tissues. In addition, overexpression of *RAMP2-AS1* led to a marked decrease in the size and weight of tumors (Fig. 6C–E). The findings suggested that the upregulation of *RAMP2-AS1* decreased the proliferation of tumor cells (Fig. 6F). Furthermore, overexpression of *RAMP2-AS1* markedly inhibited the levels of PKM2, LDHA, and HK2, and upregulated the expression of LATS2 in mice (Fig. 6G,H). Collectively, overexpression of *RAMP2-AS1* attenuated the tumorigenesis and glycolysis of NSCLC *in vivo* through upregulation of LATS2.

Discussion

Despite considerable advances, the prognosis of NSCLC has remained unsatisfactory [44]. Therefore, in-depth understanding of the mechanism of NSCLC progression and identification of new therapeutic targets are key re-

Journal of BIOLOGICAL REGULATORS and Homeostatic Agents

search imperatives. In this study, we identified downregulation of *RAMP2-AS1* in NSCLC. Further, *RAMP2-AS1* upregulation attenuated the growth and glycolysis of NSCLC via influencing LATS2-mediated Hippo signaling. In addition, FTO was found to inhibit the m^{6}A modification of *RAMP2-AS1*. These findings suggest that *RAMP2-AS1* may serve as a novel diagnostic marker and therapeutic target in NSCLC.

Glycolysis plays a crucial role in tumor development [57,58]. Exploring the relation among tumor growth and glycolysis can help better understand tumorigenesis [59, 60]. Various glycolytic enzymes are activated in tumors and cause tumor deterioration [9,61]. Lactate production is the last step in glycolysis and is associated with cancer development [58,62]. Previous studies have indicated that lncRNAs may regulate glycolysis during NSCLC development. In a previous study, lncRNA *HAR1A* was found to attenuate NSCLC progression by inhibiting glycolysis [63]. In addition, lncRNA *CYB561-5* was found to induce aerobic glycolysis and tumorigenesis of NSCLC through interacting with basigin [1]. In the present study, overexpression of *RAMP2-AS1* inhibited the glycolysis in NSCLC through mediation of Hippo signaling. To the best of our knowledge, this is the first study to suggest the role and detailed function of *RAMP2-AS1* in NSCLC.

FTO is a demethylase that serves as a vital mediator in various cancers [64,65]. The biological effects of FTO in carcinogenesis have been reported in the context of various tumors [66,67]. In addition, FTO was shown to modulate glycolysis in tumor progression by modulating RNA stability. For instance, Zhang Y *et al*. [68] found that FTO-stabilized *PRKAA1* promoted glycolysis of gastric cancer cells by controlling the redox balance. Wang H *et al*. [69] suggested that FTO-dependent m^{6}A modification may modulate the progression of endometriosis through mediation of ATG5/PKM2 axis. Consistently, in our study, FTO-mediated downregulation of *RAMP2-AS1* was found to regulate glycolysis in NSCLC cells. Mechanistically, FTO inhibited the level of *RAMP2-AS1* by downregulating the m^{6}A modification of *RAMP2-AS1* to inhibit the binding between IGF2BP2 and *RAMP2-AS1*.

LncRNAs bind with proteins and RNAs in various cancers, and they usually act as stents or guide molecules [70,71]. Additionally, KLF9 is involved in regulating glycolysis during cancer development [72,73]. In the present study, *RAMP2-AS1* was found to promote the transcriptional activation of *LATS2* through recruiting KLF9, and *RAMP2-AS1* had no influence on KLF9 level in NSCLC cells. Therefore, our findings suggest that *RAMP2-AS1* may only act as a molecular scaffold to mediate the regulatory effect of KLF9 on LATS2.

LATS2 belongs to Hippo signaling [19]. Previous studies have suggested an indispensable role of LATS2 in tumor cells [21,74]. As a tumor suppressor, LATS2 is sensitive to changes in tumor progression [75]. More importantly, upregulation of LATS2 inhibits glycolysis [76,77]. Consistently, in the present study, silencing of LATS2 abolished oe-RAMP2-AS1-induced inhibition of glycolysis in NSCLC cells. Our findings suggest a role of LATS2 in *RAMP2-AS1*-mediated glycolysis in NSCLC. *RAMP2-AS1* may inhibit glycolysis in NSCLC cells by upregulating LATS2 to modulate Hippo signaling.

Conclusion

In summary, FTO-mediated downregulation of *RAMP2-AS1* promoted aerobic glycolysis in NSCLC cells by inhibiting KLF9-mediated transcriptional activation of *LATS2*. Therefore, *RAMP2-AS1* is a potential novel therapeutic target in NSCLC.

Abbreviations

ALKBH5, alkylation repair homolog protein 5; ATP, adenosine triphosphate; BrdU, Bromodeoxyuridine; CCK-8, Cell Counting Kit-8; ChIP, Chromatin immunoprecipitation; DAPI, 4′,6-diamidino-2-phenylindole; 2-DG, 2-Deoxy-D-arabino-hexose; ECAR, Extracellular acidification rate; FISH, Fluorescence *in situ* hybridization; FITC, Fluorescein Isothiocyanate; FTO, fat mass and obesity-associated protein; GEPIA, Gene Expression Profiling Interactive Analysis; HK2, hexokinase 2; IGF2BP2, Insulin-like growth factor 2 mRNA binding protein 2; IHC, Immunohistochemistry; Ki67, antigen identified by monoclonal antibody Ki-67; KLF9, Krüppel-like factor 9; LATS2, large tumor suppressor 2; LDHA, Lactate dehydrogenase A; lncRNAs, long noncoding RNAs; LUAD, lung adenocarcinoma; LUSC, lung squamous cell carcinoma; MeRIP, M^{6}A-RNA immunoprecipitation; m^{6}A, N6-methyladenosine; NSCLC, non-small cell lung cancer; oe-NC, negative control of overexpression; PI, Propidium; PKM2, pyruvate kinase M2; RAMP2-AS1, RAMP2 antisense RNA1; RIP, RNA Immunoprecipitation; RT-qPCR, reverse transcription-quantitative polymerase chain reaction; shRNA, short hairpin RNA; SRAMP, Sequence-based RNA adenosine methylation site predictor; TAZ, Tafazzin; YAP, YES-associated protein.

Availability of Data and Materials

All experimental data included in this study can be obtained by contacting the first author if needed.

Author Contributions

YHF and SML designed this study. YHF, YMZ, LL, ZL and JWL collected the materials and performed the experiments. YHF and SML analysed the data and wrote the manuscript. SML revised the manuscript. All authors read and approved the final version of the manuscript. All au-

thors contributed to editorial changes in the manuscript. All authors have participated sufficiently in the work and agreed to be accountable for all aspects of the work.

Ethics Approval and Consent to Participate

The study protocol was reviewed by the Medical Ethics Committee of Hainan General Hospital (Hainan Affiliated Hospital of Hainan Medical University), which met the relevant national ethical requirements and agreed that the study should be conducted in accordance with the approved protocol and on the premise of informed consent, Ethics No: Med-Eth-Re [2023] 410. Each patient signed written informed consent, and the research was approved by the Ethics Committee of Hainan General Hospital (Hainan Affiliated Hospital of Hainan Medical University). Human material or human data were conducted in accordance with the Declaration of Helsinki. All animal procedures were in accordance with National Institutes of Health guidelines and approved by the Animal Care and Use Committee of Hainan General Hospital (Hainan Affiliated Hospital of Hainan Medical University) (No: Med-Eth-Re [2023] 410).

Acknowledgment

Not applicable.

Funding

This study was supported by Hainan Province Science and Technology Special Fund (Grant No. ZDYF2023SHFZ133).

Conflict of Interest

The authors declare no conflict of interest.

References

[1] Li L, Li Z, Qu J, Wei X, Suo F, Xu J, *et al*. Novel long non-coding RNA CYB561-5 promotes aerobic glycolysis and tumorigenesis by interacting with basigin in non-small cell lung cancer. Journal of Cellular and Molecular Medicine. 2022; 26: 1402–1412.

[2] Roy-Chowdhuri S. Molecular Pathology of Lung Cancer. Surgical Pathology Clinics. 2021; 14: 369–377.

[3] Musika W, Kamsa-Ard S, Jirapornkul C, Santong C, Phunmanee A. Lung Cancer Survival with Current Therapies and New Targeted Treatments: A Comprehensive Update from the Srinagarind Hospital-Based Cancer Registry from (2013 to 2017). Asian Pacific Journal of Cancer Prevention. 2021; 22: 2501–2507.

[4] Lin H, Han H, Yang M, Wen Z, Chen Q, Ma Y, *et al*. PKM2/PDK1 dual-targeted shikonin derivatives restore the sensitivity of EGFR-mutated NSCLC cells to gefitinib by remodeling glucose metabolism. European Journal of Medicinal Chemistry. 2023; 249: 115166.

[5] Li H, Huang Q, Guo H, Chen X, Li X, Qiu M. Circular RNA, circular RARS, promotes aerobic glycolysis of non-small-cell lung cancer by binding with LDHA. Thoracic Cancer. 2023; 14: 389–398.

[6] Ali T, Grote P. Beyond the RNA-dependent function of LncRNA genes. eLife. 2020; 9: e60583.

[7] Yang Z, Zhu J, Yang T, Tang W, Zheng X, Ji S, *et al*. Comprehensive analysis of the lncRNAs-related immune gene signatures and their correlation with immunotherapy in lung adenocarcinoma. British Journal of Cancer. 2023; 129: 1397–1408.

[8] Wang YW, Liu C, Chen YD, Yang B, Chen X, Ma G, *et al*. An angiogenesis-related lncRNA signature predicts the immune microenvironment and prognosis of breast cancer. Aging. 2023; 15: 7616–7636.

[9] Wang Q, Li XF, Zhou YH, Qin XH, Wang LH, Xiao MQ, *et al*. Long noncoding RNA BBOX1-AS1 increased radiotherapy sensitivity in colorectal cancer by stabilizing and activating PFK1. Translational Oncology. 2023; 36: 101751.

[10] Zhao X, Chen J, Zhang C, Xie G, Othmane B, Kuang X, *et al*. LncRNA AGAP2-AS1 interacts with IGF2BP2 to promote bladder cancer progression via regulating LRG1 mRNA stability. Cellular Signalling. 2023; 111: 110839.

[11] Cheng C, Zhang Z, Cheng F, Shao Z. Exosomal lncRNA RAMP2-AS1 Derived from Chondrosarcoma Cells Promotes Angiogenesis Through miR-2355-5p/VEGFR2 Axis. OncoTargets and Therapy. 2020; 13: 3291–3301.

[12] Li L, Gan YP, Peng H. RAMP2-AS1 inhibits CXCL11 expression to suppress malignant phenotype of breast cancer by recruiting DNMT1 and DNMT3B. Experimental Cell Research. 2022; 416: 113139.

[13] Zhou H, Guan Q, Hou X, Liu L, Zhou L, Li W, *et al*. Epithelial-mesenchymal reprogramming by KLF4-regulated Rictor expression contributes to metastasis of non-small cell lung cancer cells. International Journal of Biological Sciences. 2022; 18: 4869–4883.

[14] Sun B, Zhao J, Shao ZY. MiR-572 promotes the development of non-small cell lung cancer by targeting KLF2. European Review for Medical and Pharmacological Sciences. 2022; 26: 3083–3090.

[15] Xiao S, Jin-Xiang Y, Long T, Xiu-Rong L, Hong G, Jie-Cheng Y, *et al*. Kruppel-like factor 2 disturb non-small cell lung cancer energy metabolism by inhibited glutamine consumption. Journal of Pharmacy and Pharmacology. 2020; 72: 843–851.

[16] Hu K, Ma C, Ma R, Zheng Q, Wang Y, Zhang N, *et al*. Roles of Krüppel-like factor 6 splice variant 1 in the development, diagnosis, and possible treatment strategies for non-small cell lung cancer. American Journal of Cancer Research. 2022; 12: 4468–4482.

[17] Yu P, Cheng L, Xia WM, Liu DY, Yu JS, Zhou YF, *et al*. KLF9 inhibits the proliferation, invasion, and migration of renal cell carcinoma through the SDF-1/CXCR4 axis. The Kaohsiung Journal of Medical Sciences. 2023; 39: 587–595.

[18] Zeng FL, Lin J, Xie X, Xie YK, Zhang JH, Xu D, *et al*. LncRNA SLC7A11-AS1 promotes the progression of hepatocellular carcinoma by mediating KLF9 ubiquitination. Neoplasma. 2023; 70: 361–374.

[19] Liu L, Huang S, Du Y, Zhou H, Zhang K, He J. Lats2 deficiency protects the heart against myocardial infarction by reducing inflammation and inhibiting mitochondrial fission and STING/p65 signaling. International Journal of Biological Sciences. 2023; 19: 3428–3440.

[20] Zheng M, Li RG, Song J, Zhao X, Tang L, Erhardt S, *et al*. Hippo-Yap Signaling Maintains Sinoatrial Node Homeostasis. Circulation. 2022; 146: 1694–1711.

[21] Sun Q, Lu H, Zhang W, Du Y, Liang Q, Zhang Y, *et al*. RNF106 aggravates esophageal squamous cell carcinoma progression through LATS2/YAP axis. Archives of Biochemistry and Biophysics. 2023; 742: 109640.

[22] Cheng X, Sha M, Jiang W, Chen L, Song M. LINC00174 Suppresses Non-Small Cell Lung Cancer Progression by Up-

Journal of
BIOLOGICAL REGULATORS
and Homeostatic Agents

Regulating LATS2 via Sponging miR-31-5p. Cell Journal. 2022; 24: 140–147.

[23] Fu Y, Liu L, Wu H, Zheng Y, Zhan H, Li L. LncRNA GAS5 regulated by FTO-mediated m6A demethylation promotes autophagic cell death in NSCLC by targeting UPF1/BRD4 axis. Molecular and Cellular Biochemistry. 2023. (online ahead of print)

[24] Cheng C, Wang P, Yang Y, Du X, Xia H, Liu J, *et al*. Smoking-Induced M2-TAMs, via circEML4 in EVs, Promote the Progression of NSCLC through ALKBH5-Regulated m6A Modification of SOCS2 in NSCLC Cells. Advanced Science. 2023; 10: e2300953.

[25] Lin W, Tan ZY, Fang XC. Identification of m6A-related lncRNAs-based signature for predicting the prognosis of patients with skin cutaneous melanoma. SLAS Technology. 2024; 29: 100101.

[26] Tsim S, O'Dowd CA, Milroy R, Davidson S. Staging of non-small cell lung cancer (NSCLC): a review. Respiratory Medicine. 2010; 104: 1767–1774.

[27] Zhao L, Zhang X, Shi Y, Teng T. LncRNA SNHG14 contributes to the progression of NSCLC through miR-206/G6PD pathway. Thoracic Cancer. 2020; 11: 1202–1210.

[28] Wang R, Xing R, Su Q, Yin H, Wu D, Lv C, *et al*. Knockdown of SFRS9 Inhibits Progression of Colorectal Cancer Through Triggering Ferroptosis Mediated by GPX4 Reduction. Frontiers in Oncology. 2021; 11: 683589.

[29] Lou G, Chen L, Xia C, Wang W, Qi J, Li A, *et al*. MiR-199a-modified exosomes from adipose tissue-derived mesenchymal stem cells improve hepatocellular carcinoma chemosensitivity through mTOR pathway. Journal of Experimental & Clinical Cancer Research. 2020; 39: 4.

[30] Liang J, Liu C, Xu D, Xie K, Li A. LncRNA NEAT1 facilitates glioma progression via stabilizing PGK1. Journal of Translational Medicine. 2022; 20: 80.

[31] He C, Liu Y, Li J, Zheng X, Liang J, Cui G, *et al*. LncRNA RPSAP52 promotes cell proliferation and inhibits cell apoptosis via modulating miR-665/STAT3 in gastric cancer. Bioengineered. 2022; 13: 8699–8711.

[32] Zhu J, Tu S, Qu Q. lncRNA BZRAP1-AS1 alleviates rheumatoid arthritis by regulating miR-1286/COL5A2 axis. Immunity, Inflammation and Disease. 2022; 10: 163–174.

[33] Zhang L, Cheng H, Yue Y, Li S, Zhang D, He R. H19 knockdown suppresses proliferation and induces apoptosis by regulating miR-148b/WNT/β-catenin in ox-LDL -stimulated vascular smooth muscle cells. Journal of Biomedical Science. 2018; 25: 11.

[34] Wang X, Li Q, He S, Bai J, Ma C, Zhang L, *et al*. LncRNA FENDRR with m6A RNA methylation regulates hypoxia-induced pulmonary artery endothelial cell pyroptosis by mediating DRP1 DNA methylation. Molecular Medicine. 2022; 28: 126.

[35] Wan T, Zheng J, Yao R, Yang S, Zheng W, Zhou P. LncRNA DDX11-AS1 accelerates hepatocellular carcinoma progression via the miR-195-5p/MACC1 pathway. Annals of Hepatology. 2021; 20: 100258.

[36] Li Q, Zang Y, Sun Z, Zhang W, Liu H. Long noncoding RNA Gm44593 attenuates oxidative stress from age-related hearing loss by regulating miR-29b/WNK1. Bioengineered. 2022; 13: 573–582.

[37] Xu M, Zhou C, Weng J, Chen Z, Zhou Q, Gao J, *et al*. Tumor associated macrophages-derived exosomes facilitate hepatocellular carcinoma malignance by transferring lncMMPA to tumor cells and activating glycolysis pathway. Journal of Experimental & Clinical Cancer Research. 2022; 41: 253.

[38] Zhang H, Wang SQ, Wang L, Lin H, Zhu JB, Chen R, *et al*. m6A methyltransferase METTL3-induced lncRNA SNHG17 promotes lung adenocarcinoma gefitinib resistance by epigenetically repressing LATS2 expression. Cell Death & Disease. 2022; 13: 657.

[39] Vingiani A, Lorenzini D, Conca E, Volpi CC, Trupia DV, Gloghini A, *et al*. Pan-TRK immunohistochemistry as screening tool for NTRK fusions: A diagnostic workflow for the identification of positive patients in clinical practice. Cancer Biomarkers: Section a of Disease Markers. 2023; 38: 301–309.

[40] Yang H, Hu Y, Weng M, Liu X, Wan P, Hu Y, *et al*. Hypoxia inducible lncRNA-CBSLR modulates ferroptosis through m6A-YTHDF2-dependent modulation of CBS in gastric cancer. Journal of Advanced Research. 2021; 37: 91–106.

[41] Li T, Hu PS, Zuo Z, Lin JF, Li X, Wu QN, *et al*. METTL3 facilitates tumor progression via an m^6A-IGF2BP2-dependent mechanism in colorectal carcinoma. Molecular Cancer. 2019; 18: 112.

[42] Zhou L, Jiang J, Huang Z, Jin P, Peng L, Luo M, *et al*. Hypoxia-induced lncRNA STEAP3-AS1 activates Wnt/β-catenin signaling to promote colorectal cancer progression by preventing m^6A-mediated degradation of STEAP3 mRNA. Molecular Cancer. 2022; 21: 168.

[43] Yuan K, Lan J, Xu L, Feng X, Liao H, Xie K, *et al*. Long noncoding RNA TLNC1 promotes the growth and metastasis of liver cancer via inhibition of p53 signaling. Molecular Cancer. 2022; 21: 105.

[44] Yang Q, Wang M, Xu J, Yu D, Li Y, Chen Y, *et al*. LINC02159 promotes non-small cell lung cancer progression via ALYREF/YAP1 signaling. Molecular Cancer. 2023; 22: 122.

[45] Luo Y, Zheng S, Wu Q, Wu J, Zhou R, Wang C, *et al*. Long noncoding RNA (lncRNA) *EIF3J-DT* induces chemoresistance of gastric cancer via autophagy activation. Autophagy. 2021; 17: 4083–4101.

[46] Chen S, Zhang Y, Ding X, Li W. Identification of lncRNA/circRNA-miRNA-mRNA ceRNA Network as Biomarkers for Hepatocellular Carcinoma. Frontiers in Genetics. 2022; 13: 838869.

[47] Aydinli M, Liang C, Dandekar T. Motif and conserved module analysis in DNA (promoters, enhancers) and RNA (lncRNA, mRNA) using AlModules. Scientific Reports. 2022; 12: 17588.

[48] Shen W, Pu J, Zuo Z, Gu S, Sun J, Tan B, *et al*. The RNA demethylase ALKBH5 promotes the progression and angiogenesis of lung cancer by regulating the stability of the LncRNA PVT1. Cancer Cell International. 2022; 22: 353.

[49] Ma Y, Yu L, Yan W, Qiu L, Zhang J, Jia X. lncRNA GAS5 Sensitizes Breast Cancer Cells to Ionizing Radiation by Inhibiting DNA Repair. BioMed Research International. 2022; 2022: 1987519.

[50] Song Z, Zhang Y, Chen Z, Zhang B. Identification of key genes in lung adenocarcinoma based on a competing endogenous RNA network. Oncology Letters. 2021; 21: 60.

[51] Li J, Cao H, Yang J, Wang B. CircCDK1 blocking IGF2BP2-mediated m6A modification of CPPED1 promotes laryngeal squamous cell carcinoma metastasis via the PI3K/AKT signal pathway. Gene. 2023; 884: 147686.

[52] Zhang J, Bai S, Yan Y, Kang H, Li G, Feng Z, *et al*. Construction of lncRNA-m6A gene-mRNA regulatory network to identify m6A-related lncRNAs associated with the progression of lung adenocarcinoma. BMC Pulmonary Medicine. 2023; 23: 284.

[53] Jiang X, Liu B, Nie Z, Duan L, Xiong Q, Jin Z, *et al*. The role of m6A modification in the biological functions and diseases. Signal Transduction and Targeted Therapy. 2021; 6: 74.

[54] Ganapathy-Kanniappan S, Geschwind JFH. Tumor glycolysis as a target for cancer therapy: progress and prospects. Molecular Cancer. 2013; 12: 152.

[55] Li Y, Sun Q, Jiang M, Li S, Zhang J, Xu Z, *et al*. KLF9 sup-

presses gastric cancer cell invasion and metastasis through transcriptional inhibition of MMP28. FASEB Journal. 2019; 33: 7915–7928.

[56] Fang QY, Deng QF, Luo J, Zhou CC. MiRNA-20a-5p accelerates the proliferation and invasion of non-small cell lung cancer by targeting and downregulating KLF9. European Review for Medical and Pharmacological Sciences. 2020; 24: 2548–2556.

[57] Ding Z, Yang J, Wu B, Wu Y, Guo F. Long non-coding RNA CCHE1 modulates LDHA-mediated glycolysis and confers chemoresistance to melanoma cells. Cancer & Metabolism. 2023; 11: 10.

[58] Wang T, Zhu X, Wang K, Ding R. Circ_0006324 regulates cell proliferation, cell-cycle progression, apoptosis, and glycolysis of non-small cell lung cancer cells through miR-496/TRIM59 axis. Journal of Biochemical and Molecular Toxicology. 2023; 37: e23473.

[59] Mirzaei S, Ranjbar B, Tackallou SH. Molecular profile of non-coding RNA-mediated glycolysis control in human cancers. Pathology - Research and Practice. 2023; 248: 154708.

[60] Khorsand M, Mostafavi-Pour Z, Tahmasebi A, Omidvar Kordshouli S, Mousavi P. Construction of lncRNA/Pseudogene-miRNA Network Based on In Silico Approaches for Glycolysis Pathway to Identify Prostate Adenocarcinoma-Related Potential Biomarkers. Applied Biochemistry and Biotechnology. 2023; 1–24.

[61] Xu H, Ba Z, Liu C, Yu X. Long noncoding RNA DLEU1 promotes proliferation and glycolysis of gastric cancer cells via APOC1 upregulation by recruiting SMYD2 to induce trimethylation of H3K4 modification. Translational Oncology. 2023; 36: 101731.

[62] Wang D, Qiu B, Liu Q, Xia L, Liu S, Zheng C, *et al*. Patlak-Ki derived from ultra-high sensitivity dynamic total body [^{18}F]FDG PET/CT correlates with the response to induction immunochemotherapy in locally advanced non-small cell lung cancer patients. European Journal of Nuclear Medicine and Molecular Imaging. 2023; 50: 3400–3413.

[63] Ma J, Cao K, Ling X, Zhang P, Zhu J. LncRNA HAR1A Suppresses the Development of Non-Small Cell Lung Cancer by Inactivating the STAT3 Pathway. Cancers. 2022; 14: 2845.

[64] Yang X, Qiao S, Zhao W, Li S, Qiao Y, Jiang Y, *et al*. Homogeneous Electrochemiluminescence for Highly Sensitive Determination of Demethylase FTO Based on Target-Regulated DNAzyme Cleavage and Host-Guest Interaction. Analytical Chemistry. 2023; 95: 11420–11428.

[65] Zhang J, Wei J, Sun R, Sheng H, Yin K, Pan Y, *et al*. A lncRNA from the FTO locus acts as a suppressor of the m^{6}A writer complex and p53 tumor suppression signaling. Molecular Cell. 2023; 83: 2692–2708.e7.

[66] Xiao P, Duan Z, Liu Z, Chen L, Zhang D, Liu L, *et al*. Rational Design of RNA Demethylase FTO Inhibitors with Enhanced Antileukemia Drug-Like Properties. Journal of Medicinal Chemistry. 2023; 66: 9731–9752.

[67] Wang A, Jin C, Wang Y, Yu J, Wang R, Tian X. FTO promotes the progression of cervical cancer by regulating the N6-methyladenosine modification of ZEB1 and Myc. Molecular Carcinogenesis. 2023; 62: 1228–1237.

[68] Zhang Y, Zhou X, Cheng X, Hong X, Jiang X, Jing G, *et al*. PRKAA1, stabilized by FTO in an m6A-YTHDF2-dependent manner, promotes cell proliferation and glycolysis of gastric cancer by regulating the redox balance. Neoplasma. 2022; 69: 1338–1348.

[69] Wang H, Liang Z, Gou Y, Li Z, Cao Y, Jiao N, *et al*. FTO-dependent N(6)-Methyladenosine regulates the progression of endometriosis via the ATG5/PKM2 Axis. Cellular Signalling. 2022; 98: 110406.

[70] Shi Z, Zhang H, Shen Y, Zhang S, Zhang X, Xu Y, *et al*. SETD1A-mediated H3K4me3 methylation upregulates lncRNA HOXC-AS3 and the binding of HOXC-AS3 to EP300 and increases EP300 stability to suppress the ferroptosis of NSCLC cells. Thoracic Cancer. 2023; 14: 2579–2590.

[71] Wheeler BD, Gagnon JD, Zhu WS, Muñoz-Sandoval P, Wong SK, Simeonov DS, *et al*. The lncRNA *Malat1* inhibits miR-15/16 to enhance cytotoxic T cell activation and memory cell formation. eLife. 2023; 12: RP87900.

[72] Xing J, Jia Z, Xu Y, Chen M, Yang Z, Chen Y, *et al*. KLF9 (Kruppel Like Factor 9) induced PFKFB3 (6-Phosphofructo-2-Kinase/Fructose-2, 6-Biphosphatase 3) downregulation inhibits the proliferation, metastasis and aerobic glycolysis of cutaneous squamous cell carcinoma cells. Bioengineered. 2021; 12: 7563–7576.

[73] Jin Y, Xu L, Zhao B, Bao W, Ye Y, Tong Y, *et al*. Tumour-suppressing functions of the lncRNA MBNL1-AS1/miR-889-3p/KLF9 axis in human breast cancer cells. Cell Cycle. 2022; 21: 908–920.

[74] Sahu RK, Ruhi S, Jeppu AK, Al-Goshae HA, Syed A, Nagdev S, *et al*. Malignant mesothelioma tumours: molecular pathogenesis, diagnosis, and therapies accompanying clinical studies. Frontiers in Oncology. 2023; 13: 1204722.

[75] Sato T, Akao K, Sato A, Tsujimura T, Mukai S, Sekido Y. Aberrant expression of NPPB through YAP1 and TAZ activation in mesothelioma with Hippo pathway gene alterations. Cancer Medicine. 2023; 12: 13586–13598.

[76] Jiang SF, Li RR. hsa_circ_0067514 suppresses gastric cancer progression and glycolysis via miR-654-3p/LATS2 axis. Neoplasma. 2022; 69: 1079–1091.

[77] Liu F, Wu H, Wu G, Long J, Dai J, Wang Z. circPKD2 inhibits the glioma cell proliferation, invasion and glycolytic metabolism through regulating the miR-1278/LATS2 axis. Neuroscience Letters. 2023; 801: 137126.